SCIENTIFIC REPORTS

OPEN

SUBJECT AREAS:
PATTERN RECOGNITION RECEPTORS
INFECTION
IMMUNOCHEMISTRY
ADAPTIVE IMMUNITY

Received
13 May 2013

Accepted
13 December 2013

Published
14 January 2014

Correspondence and requests for materials should be addressed to J.L.D. (dbsdjl@nus.edu.sg)

* Current address: FIMS & BJRC, The 1st Affiliated Hospital and Frontier Institute of Science and Technology, Xi'an Jiaotong University, Xi'an, China, 710061.

† Current address: School of Biological Sciences, Nanyang Technological University, 60 Nanyang Drive, Singapore 637511.

# Molecular interaction between natural IgG and ficolin – mechanistic insights on adaptive-innate immune crosstalk

Saswati Panda[1], Jing Zhang[2]*, Lifeng Yang[3]†, Ganesh S. Anand[1] & Jeak L. Ding[1,3]

[1]Department of Biological Sciences, Faculty of Science, National University of Singapore, Singapore, 117543, [2]NUS graduate School for Integrative Science and Engineering, National University of Singapore, Singapore, 117543, [3]Computational and Systems Biology, Singapore-MIT Alliance, 4 Engineering Drive 3, Singapore, 117576.

**Recently, we found that natural IgG (nIgG; a non-specific immunoglobulin of adaptive immunity) is not quiescent, but plays a crucial role in immediate immune defense by collaborating with ficolin (an innate immune protein). However, how the nIgG and ficolin interplay and what factors control the complex formation during infection is unknown. Here, we found that mild acidosis and hypocalcaemia induced by infection- inflammation condition increased the nIgG:ficolin complex formation. Hydrogen-deuterium exchange mass spectrometry delineated the binding interfaces to the CH2–CH3 region of nIgG Fc and P-subdomain of ficolin FBG domain. Infection condition exposes novel binding sites. Site-directed mutagenesis and surface plasmon resonance analyses of peptides, derived from nIgG and ficolin, defined the interacting residues between the proteins. These results provide mechanistic insights on the interaction between two molecules representing the adaptive and innate immune pathways, prompting potential development of immunomodulatory/prophylactic peptides tunable to prevailing infection conditions.**

In order to combat pathogens, the host has evolved an elaborate immune system comprising of two arms: innate and adaptive[1], which are conventionally known to act in a biphasic manner. Although appearing separate and sequential, the interaction between proteins of the innate and adaptive immune pathways has been shown to shape the adaptive immune response[2]. For example, mannose binding lectin (MBL, a soluble innate immune PPR) binds to adaptive immune molecules such as antigen-specific IgG in immune complexes[3], antigen-specific IgM[4] and secretory IgA[5], to facilitate the clearance of the opsonized microbes through activation of the complement pathway and prime the subsequent adaptive response. However, little is known about the molecular mechanisms by which adaptive immunity may fine-tune the innate immune responses, since the latter is deemed to be the frontline defense. The potential interactions between the proteins of the adaptive and innate arms of immunity remain an important area to be explored.

In contrast to the well-known antigen-specific antibodies that are produced specifically during the adaptive immune response to an infection, there is a pool of non-specific naturally occurring antibodies comprising of IgM, IgG and IgA subtypes, which exists prior to an external infection. Amongst the natural antibody isotypes, the natural IgM has been most well-studied. The natural IgM was shown to possess non-specific avidity for pathogens, by virtue of its pentameric structure[6,7], which enables it to exhibit a protective effect during infections[8,9]. Natural IgG (henceforth referred to as nIgG) belongs to the IgG3 subclass. Although nIgG makes up the majority of the serum natural antibodies[10,11], the significance of its existence and function remained unexplored. Recently, Panda et al[12] showed that nIgG (deemed to be an adaptive immune protein) collaborates with major serum lectins like ficolin and MBL, to immediately elicit host defense. It was demonstrated that nIgG specifically collaborates with ficolin (a pattern recognition receptor belonging to the lectin family of soluble PRRs) that is pre-bound to the pathogen, resulting in effective recognition and opsonization of the invading pathogen. The resulting nIgG:ficolin immune complex bound on the pathogen evokes innate immune defense, clearing the pathogen through FcγR1-mediated phagocytosis. The H-ficolin was shown to be the most effective of the ficolin isoforms. Further *in vivo* studies demonstrated the protective role of nIgG. Mice lacking nIgG showed significantly higher bacterial burdens in the tissues, delay in bacterial clearance, increased pro-inflammatory and lowered anti-inflammatory cytokine production and compromised survival post-infection. Reconstitution with nIgG restored nIgG:ficolin mediated bacterial recognition and clearance and improved survival[12]. These findings prompted us to probe the dynamics of nIgG:ficolin interaction during an infection.

In this study, we explored the interaction between the nIgG and H-ficolin under simulated physiological (pH 7.4, 2.5 mM calcium) and infection-inflammation (pH 6.5, 2.0 mM calcium) conditions. We showed that the Fc domain of nIgG specifically interacts with the FBG domain of ficolin. We further delineated the specific binding interfaces and peptides involved in interaction under normal and infection-inflammation conditions. Specific arginine and lysine residues were identified to be responsible for regulating basal interaction under normal condition, whereas histidine appeared to be crucial in increasing the affinity of nIgG:ficolin interaction under the infection-inflammation condition. Our results reveal novel insights into how adaptive immunity shapes innate immunity through molecular crosstalk between the proteins of the two arms of immunity. Identification of the cognate interactive peptides prompts future development of immunomodulators, which are tunable by pH and calcium changes in the microenvironment of infection.

## Results

**Natural IgG complexes with ficolin to recognize bacteria during infection.** Recently, we found that nIgG (belonging to the IgG3 subclass), present in the uninfected serum and deemed to be inactive[10,11], actually plays an important role in the immediate microbial recognition and clearance. It does so with the aid of ficolin[12]. This was further supported by specific interactions occurring between representative nIgGs (human anti-alpha gal IgG[13] and IgG3 from T-cell deficient mice[14]) and pathogen-associated ficolin. This novel finding of an adaptive immune molecule collaborating with innate immune proteins and contributing to an immediate immune defense sheds light on the underestimated role of natural antibodies, and prompted us to further examine the nIgG:ficolin interaction during infection[12,15]. We found that nIgG alone (purified from the sera of previously uninfected mice) could not recognize *Pseudomonas aeruginosa* (Fig. 1a). However, nIgG was recruited significantly and in a dose-dependent manner in the presence of serum depleted of IgG ($IgG^-$ serum). This indicates that other serum factors probably facilitated the bacterial recognition ability of nIgG. Since our recent study revealed ficolin to be an important player in enabling bacterial recognition by nIgG[12], we further depleted ficolin from the $IgG^-$ serum and found that nIgG recruitment to the bacteria was significantly reduced, suggesting that ficolin is a crucial serum factor, which enables nIgG deposition on the bacteria (Fig. 1a).

Next, we tested the uptake of the bacteria opsonized by nIgG:ficolin immune complexes, by monocytes. Our earlier study showed that amongst all the ficolin isoforms (L-, H- and M-ficolin) tested, H-ficolin enabled maximal uptake of nIgG opsonized bacteria[12]. Hence, we focused on the biological effects of nIgG:H-ficolin complex-opsonization of the bacterial mimic (GlcNAc-beads). N-acetyl glucosamine (GlcNAc) is a pathogen-associated molecular pattern (PAMP) specifically recognized by ficolin. We found that GlcNAc-beads opsonized with H-ficolin alone were not recognized by the U937 monocytes. However, pre-incubation of the GlcNAc-beads with nIgG and H-ficolin led to efficient opsonization and co-localization of the nIgG:H-ficolin immune complex on the monocytes (Fig. 1b).

Infection-induced inflammation is known to cause a drop in pH[16–18] and calcium[19–21] levels in the serum at the microenvironment of the infection site. This is known to boost the interaction between the immune proteins and subsequent anti-microbial response[22]. This prompted us to explore the extent of nIgG:H-ficolin interaction under simulated physiological condition (pH 7.4 and 2.5 mM $Ca^{2+}$) and infection-inflammation condition (pH 6.5 and 2 mM $Ca^{2+}$). For this purpose, we used specific buffers previously established by others who also used these conditions to study protein:protein interaction in innate immune response[22–24]. To support our observation of nIgG:H-ficolin immune complex formation (Fig. 1b) we enumerated the immune complexes formed under the normal and infection-inflammation conditions by using proximity ligation assay (PLA) to demonstrate the nIgG:H-ficolin interactions *in situ*. Upon incubating the monocytes with the nIgG:H-ficolin opsonized GlcNAc-beads, we observed a significant increase in the number of complexes (each red dot signifies a complex) under the infection-inflammation condition as compared to the normal condition (Fig. 1c, d). These results highlight the importance of the molecular interaction between nIgG and H-ficolin (wherein ficolin is pre-bound to the bacteria), and emphasize the bridging action of nIgG in bringing the H-ficolin-bound bacteria to the monocytes for clearance. The marked increase in the nIgG:H-ficolin immune complex formation under infection-inflammation condition also suggests that this immune response is specific, biophysically stable and ensures no random over-activation of the immune reaction, although a basal level of nIgG:ficolin immune complex formation occurs under normal condition.

**nIgG:ficolin immune complexes are increased by infection.** After ascertaining that nIgG:ficolin immune complexes direct the opsonized bacteria to the monocytes *in vitro*, we explored whether nIgG:ficolin complexes are formed *in vivo* in mice, post-infection. We observed an increase in the nIgG:ficolin complexes in a time (0–24 hours post-infection, hpi)- and dose ($10^6$–$10^7$ cfu)- dependent manner (Fig. 2a) in the serum of mice infected with *Pseudomonas aeruginosa*. As immune complexes are known to be targeted to the spleen to prevent the spread of infection to other vital organs[25], we checked for presence of nIgG:ficolin complexes in the spleens of infected mice. A corresponding increase in nIgG:ficolin complexes was observed in a dose- and time- dependent manner (Fig. 2b), concurrent with the increase in complex formation observed in the serum (Fig. 2a). This further supports the stability of the nIgG:ficolin complexes and their pathophysiological significance.

To gain further insights into the mode of nIgG:ficolin interaction, we characterized and delineated the dynamics of nIgG:ficolin interaction. Since there are three isoforms of ficolin, each comprising a collagen-like domain[26,27] and a fibrinogen-like domain (FBG), which recognizes PAMPs like GlcNAc, it was pertinent for us to check the interaction of nIgG with all three ficolin isoforms. By yeast 2-hybrid assay, we observed that nIgG interacted with all three ficolin isoforms, showing strongest interaction with H-ficolin (Fig. 2c). We observed higher binding preference between nIgG and H-ficolin.

**The CH2–CH3 subdomain of nIgG Fc interacts with the P-subdomain of ficolin FBG.** Next, we characterized the domain-specific interaction between nIgG and ficolin by studying the subdomain-specific interaction of the two proteins in comparison with their respective full-length proteins. We observed that nIgG Fc region interacts with the FBG domain of ficolin (Fig. 3a). The negative controls showed no interaction, ascertaining the specificity of nIgG Fc:ficolin FBG interaction. We found that nIgG purified from uninfected human serum (Supplementary fig. 1a, b) bound dose-dependently to the ficolin FBG domain immobilized on GlcNAc-BSA (Fig. 3b). In particular, significantly stronger binding between nIgG and ficolin FBG was observed under infection-inflammation condition (Fig. 3b).

Since we have delineated the nIgG:ficolin interaction to the Fc region of nIgG and the FBG domain of ficolin (Fig. 3), and that the infection-inflammation condition increases the nIgG:ficolin complex formation (Fig. 3b), it was imperative to locate their precise binding interfaces under normal and infection-inflammation conditions to gain further insights into the dynamics of interaction during an infection. We mapped the interaction sites using amide hydrogen-deuterium exchange coupled with mass spectrometry (HDMS). A reduction in deuterium incorporation in the presence of a protein partner indicates that the corresponding specific peptide sequence is involved in the interaction surface[28,29]. The differential incorporation

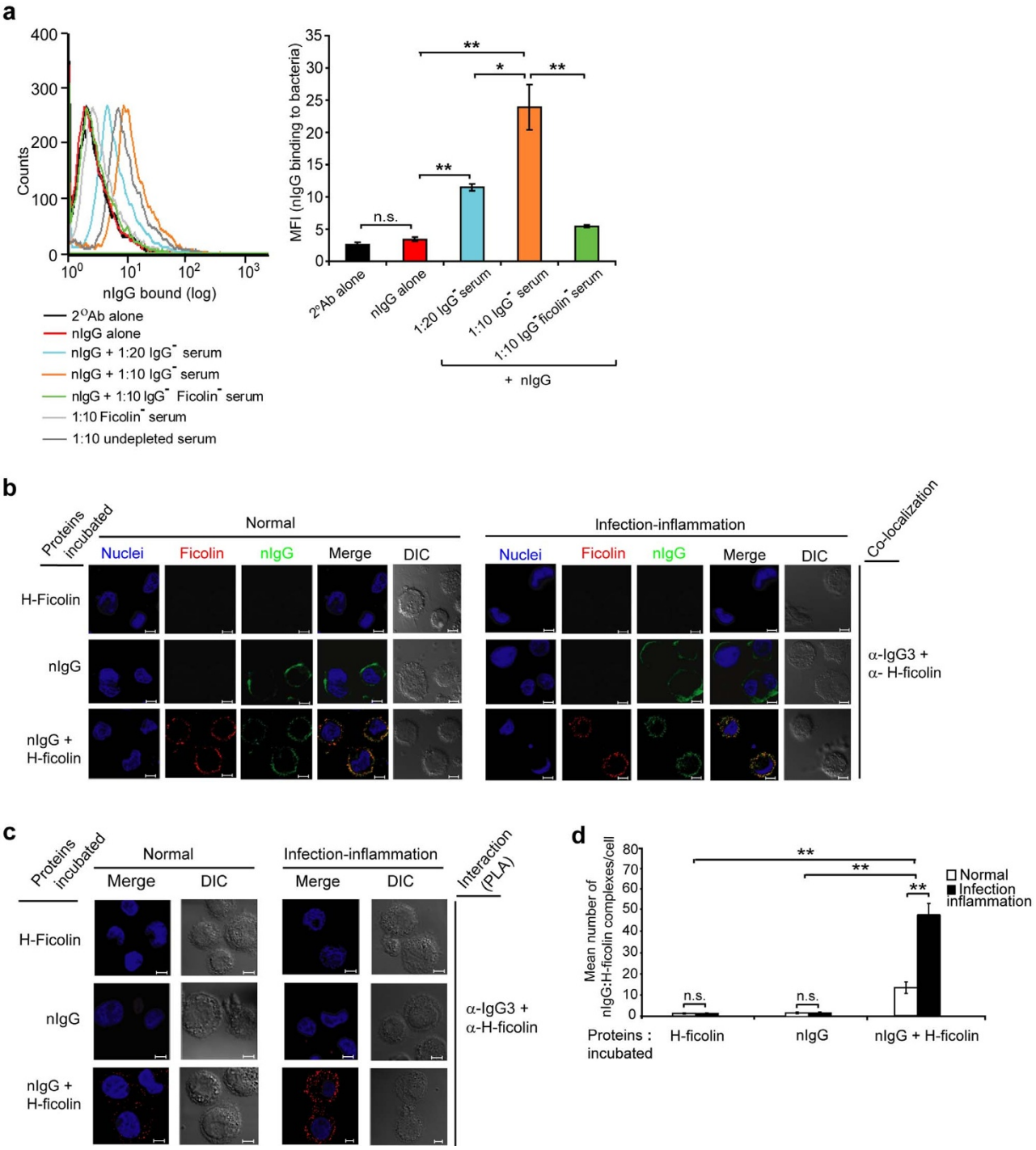


**Figure 1 | Natural IgG collaborates with ficolin to recognize bacteria and form immune complexes on monocytes.** (a) FACS analysis to detect nIgG bound to $10^6$ cfu *P. aeruginosa* opsonized with proteins (see key below the figure) and incubated with primary anti-mouse IgG3, followed by staining with Alexa488-conjugated secondary antibody. nIgG purified from undepleted pooled sera of uninfected mice (n = 8) does not bind to *P. aeruginosa* (red). It binds to the bacteria only when aided by dose-dependent increase in $IgG^-$ serum (1 : 20; blue and 1 : 10; orange). Further depletion of ficolin from the $IgG^-$ serum (1 : 10 $ficolin^-$ $IgG^-$ serum; green) shows reduction in binding of nIgG to *P. aeruginosa*. nIgG binding decreases when bacteria were incubated with 1 : 10 $ficolin^-$ serum (light grey) as compared to 1 : 10 undepleted serum (dark grey), indicated by the shift (arrow). The right panel shows quantitative comparison of the FACS plots of different samples indicated by mean fluorescence intensity (MFI) of nIgG binding. (b–d) U937 monocytes were incubated with GlcNac-beads opsonized with H-ficolin, nIgG or the nIgG:ficolin complex. (b) Confocal microscopy to detect co-localization of nIgG (green) and ficolin (red) on the monocytes, which were pre-incubated for 30 min at room temperature with GlcNAc-beads opsonized with H-ficolin, nIgG or the nIgG:H-ficolin complex. The cell nuclei were stained with DAPI (blue). 63× objective; scale bar, 5 μm. (c) *In situ* proximity ligation assay (PLA) to identify nIgG:ficolin interaction under normal and infection-inflammation conditions on the monocytes, using anti-human IgG3 and anti-H-ficolin antibodies. Protein-protein interactions are seen as PLA signals – each red dot represents an interaction. 63× objective; scale bar, 5 μm. (d) Quantification of the number of PLA signals of nIgG:H-ficolin complex. The interaction complexes per cell were scored using Image J software. Duplicates of 50 cells each were enumerated for each condition tested. Three replicates per condition were tested and three independent experiments were performed. $*p < 0.05$; $**p < 0.01$; n.s., not significant.

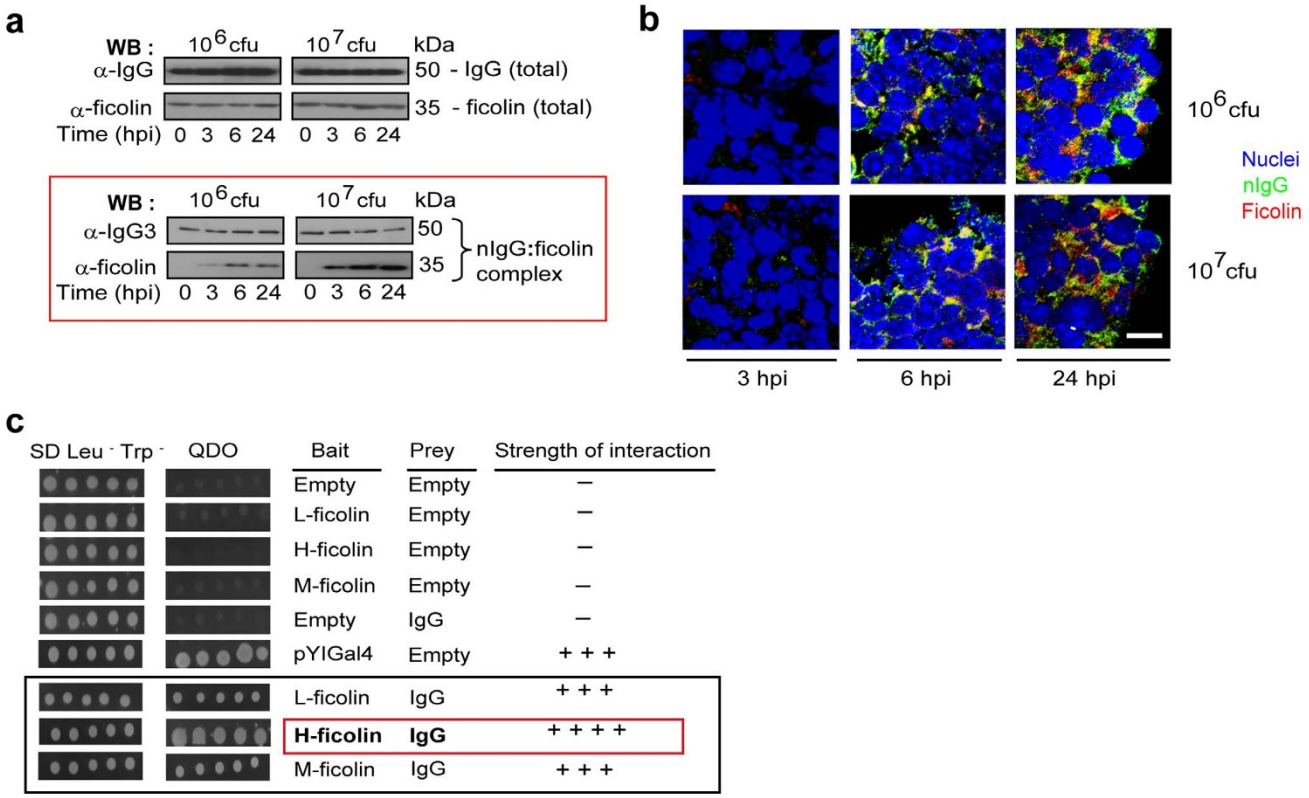


**Figure 2 | nIgG:ficolin immune complexes increase post-infection.** (a) Immunoblot analysis of total IgG (50 kDa heavy chain) and ficolin levels in the pooled sera of mice (n = 8) (top panel) and detection of nIgG (50 kDa heavy chain of mouse IgG3) and ficolin in nIgG:ficolin complexes (pulled down by Protein G beads) in serum (boxed in red), post-infection with $10^6$ or $10^7$ cfu *P. aeruginosa* over time course. The samples were derived from the same experiment, resolved under 12% reducing SDS-PAGE and the gels and blots were processed in parallel. Representative immunoblots (cropped for improving clarity and conciseness of presentation) from three independent experiments is shown. Full-length blots are presented in Supplementary Fig. 4a. (b) Immunofluorescence staining to detect co-localization of nIgG:ficolin complexes (using anti-mouse IgG3 and anti-ficolin) in spleen sections of WT mice (n = 3), infected with $10^6$ or $10^7$ cfu *P. aeruginosa* over time course. 100× objective. Scale bars, 10 μm. (c) Yeast two-hybrid screening to detect single chain interaction between nIgG and L-, H- and M-ficolin isoforms. nIgG interacts strongest with H-ficolin (red box).

of deuterium for each peptide was calculated across all time points of interaction.

We determined the contact surfaces on the nIgG molecule when complexed with H-ficolin. The nIgG peptides: DTLMISRTPEVTCVV$^{278–292}$, VLHQDWLNGKE$^{337–347}$ and LTCLVKGFYPSDI$^{394–406}$, corresponding to the CH2–CH3 interface in the Fc region showed decreased deuterium incorporation in the presence of H-ficolin (Fig. 4a [i] and 4b). The non-binding nIgG peptides, which show no difference in deuterium incorporation in the presence or absence of H-ficolin, are the negative control peptides (Fig. 4a [ii]). When we compared the extent of deuterium incorporation in H-ficolin alone and H-ficolin incubated with nIgG under normal condition, we found three interacting peptides in the P subdomain of ficolin FBG domain: YRAGFGNQESEFWLGNENLHQ$^{150–170}$, AHYATFRLLGEVDHYQL$^{193–209}$ and NGRYAVSEAAAHKYGID$^{264–280}$, which showed marked differences in deuterium incorporation when in complex with nIgG (Fig. 4c [i] and 4d). These observations are consistent with the ELISA results (Fig. 3b), which also indicated that ficolin FBG harbors the binding sites for nIgG.

Interestingly, an additional H-ficolin peptide, YDADHDSSNSNC$^{234–245}$ (Fig. 4c [i] lower panel), also in the P subdomain of FBG, showed decreased deuterium uptake under the infection-inflammation condition. This supports our postulate that an infection-induced reduction in pH may expose additional sites in the ficolin for the nIgG to bind to, and it also supports the 100-fold increase in affinity between nIgG and H-ficolin FBG under infection-inflammation condition[12]. In addition under the infection-inflammation condition, the nIgG:H-ficolin complex exhibited four FBG peptides spanning residues PRNCRELLS$^{90–98}$, YHLCLPEGR$^{107–115}$, QRRQDGSVDFFR$^{134–145}$ and GVGHPYRRVRMM$^{286–297}$, each showing increased deuterium uptake (Fig. 4c [ii] ), indicating greater solvent accessibility under reduced pH and calcium conditions. The H-ficolin peptides showing no difference in deuterium incorporation in the presence or absence of nIgG are the non-binding control peptides (Fig. 4c [iii]).

We also performed computational docking studies between IgG Fc (PDB code: 1H3Y) and ficolin FBG (PDB code: 2J64) using either random (Supplementary fig. 2a) or guided docking based on the HDMS results (Supplementary fig. 2b). The HDMS-guided docking showed a lower energy score (ZRank score) compared to random docking (Supplementary fig. 2c), which indicates higher stability and better probability of complex formation.

**Histidine is the critical residue regulating infection-inflammation induced nIgG:ficolin interaction.** Next, to further understand how perturbation of the micro-environment at the site of infection affects the nIgG:ficolin interaction (which has implications on how the adaptive and innate immune systems crosstalk at a molecular level), we attempted to define the precise binding residues between nIgG and ficolin. Based on the HDMS results, we synthesized peptides derived from nIgG and ficolin, and performed surface plasmon resonance (SPR) analysis to characterize the real-time interaction between these peptides and their cognate proteins (ficolin or nIgG, respectively) under normal and infection-inflammation conditions. We also tested single- and double- amino acid mutant peptides, where arginine (R), lysine (K) and histidine (H) were

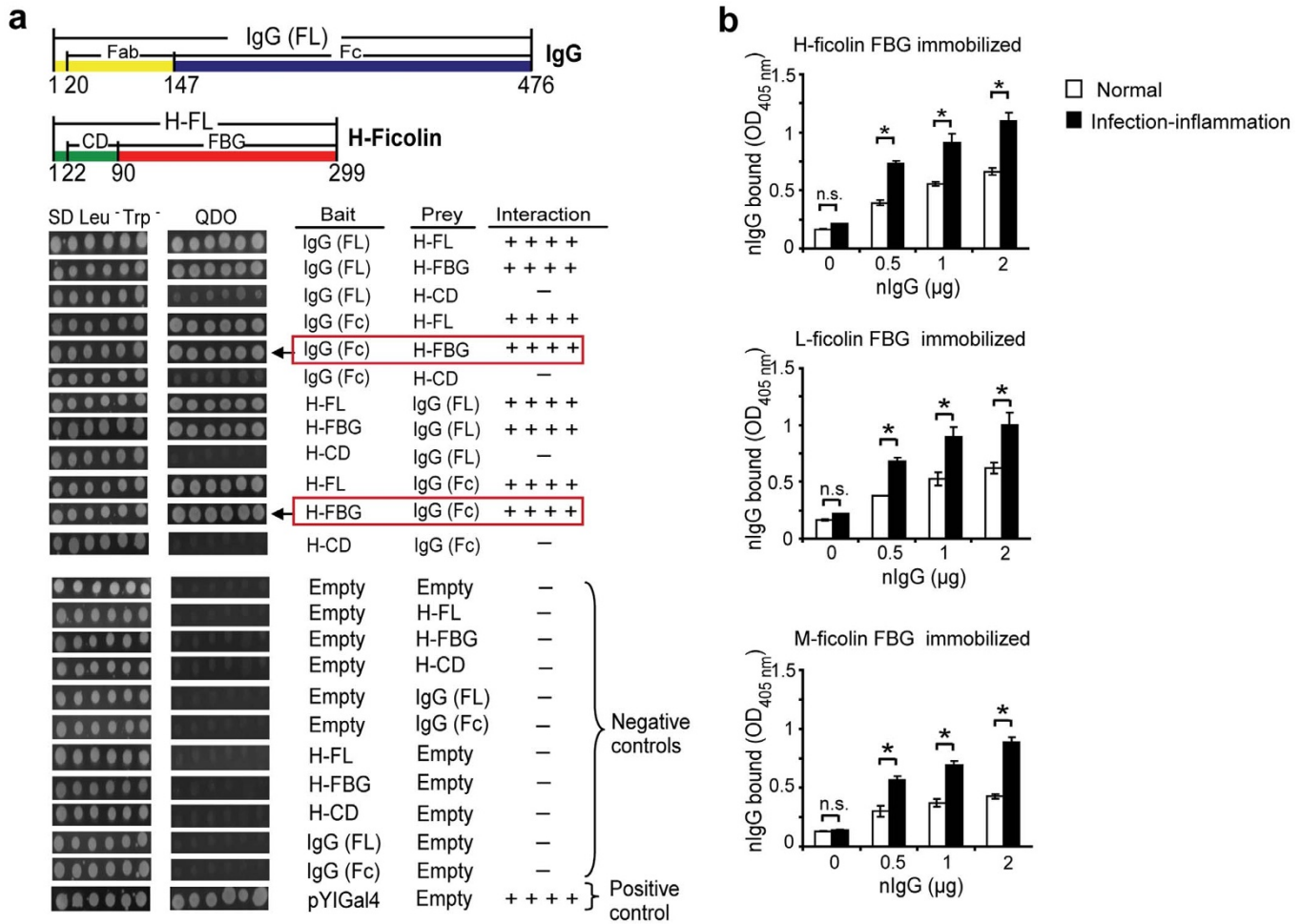


**Figure 3 | nIgG Fc interacts with ficolin FBG – infection-inflammation condition increases IgG:ficolin complex formation.** (a) Delineation of the single chain interaction domains of nIgG and H-ficolin by yeast two-hybrid. The full-length and Fc region of nIgG and the full-length, FBG and collagen-like domain of H-ficolin were individually subcloned into the bait and prey vectors. To compare the strength of interaction, yeast colonies were serially diluted and plated on QDO plates. Either in bait or prey vectors, nIgG Fc exhibited strongest interaction with FBG domain of H-ficolin (red boxes). (b) ELISA to detect binding of nIgG purified from uninfected human serum to recombinant L-, H- and M-ficolin FBG bound on immobilized GlcNAc-BSA under both normal (white bar) and infection-inflammation (black bar) conditions. Firstly, ficolin FBG was incubated with immobilized GlcNAc-BSA, followed by increasing doses of purified IgG. nIgG bound was detected using anti-human IgG3 and corresponding HRP-conjugated secondary antibody. Absorbance (OD) was read at 405 nm. Three replicates per condition were tested and three independent experiments were performed. $*p < 0.05$; $**p < 0.01$; n.s., not significant.

substituted with uncharged alanine (A). We found that the nIgG peptides, DTLMISRTPEVTCVV$^{278–292}$ (peptide 1) and LTCLVKGFYPSDI$^{394–406}$ (peptide 6) bound to ficolin on GlcNAc-chip with similar affinity ($K_D \sim 10^{-6}$ M) under both normal and infection-inflammation conditions (Fig. 5). However, the binding was abolished by a point mutation of R (peptide 2) or K (peptide 7) to an uncharged A residue. Moreover, a mutation from H-A (VLAQDWLNGKE, peptide 4) abolished the interaction between this nIgG peptide and ficolin at pH 6.5. The wild type peptide (VLHQDWLNGKE$^{337–347}$, peptide 3) and the K-A substitution mutant (VLHQDWLNGAE, peptide 5), both interacted with ficolin at higher affinity under infection-inflammation condition as compared to the normal condition, indicating that K$^{346}$ is not a critical residue involved in interaction. Taken together, our results suggest that the interaction between nIgG:ficolin is controlled by electrostatic forces between charged side chains of amino acids - Arg and Lys regulate a basal level of interaction under normal condition whereas, Arg, Lys and His regulate interaction under infection-inflammation condition. The mutant nIgG peptides (2,4,5,7) did not bind to ficolin under both normal and infection-inflammation conditions. Sensorgrams for peptides 3 and 5, tested under normal condition, are shown as representative non-binding SPR plots. On the whole, we have found that multiple positively charged side chains of Arg and Lys contributed to basal binding affinity under normal condition, while His$^{339}$ specifically contributed to higher affinity under infection-inflammation condition (Fig. 5).

**nIgG peptides block the formation of nIgG:ficolin complex under infection condition.** Next, we examined whether the peptides derived from nIgG would affect nIgG:ficolin complex formation under infection condition. To achieve this, we first tested the binding of nIgG to ficolin bound to GlcNAc in the absence or presence of increasing doses of three "ficolin-binding nIgG peptides" (an equimolar mixture of DTLMISRTPEVTCVV$^{278–292}$, VLHQDWLNGKE$^{337–347}$ and LTCLVKGFYPSDI$^{394–406}$ in 1 : 1 or 5 : 1 molar ratio of nIgG peptides to ficolin). We also compared nIgG:ficolin complex formation in the presence of non-binding mutant nIgG peptides (DTLMISATPEVTCVV$^{278–292}$, VLAQDWLNGKE$^{337–347}$ and LTCLVAGFYPSDI$^{394–406}$) as a control. Figure 6a shows successive reduction in the levels of nIgG bound to ficolin when co-incubated with

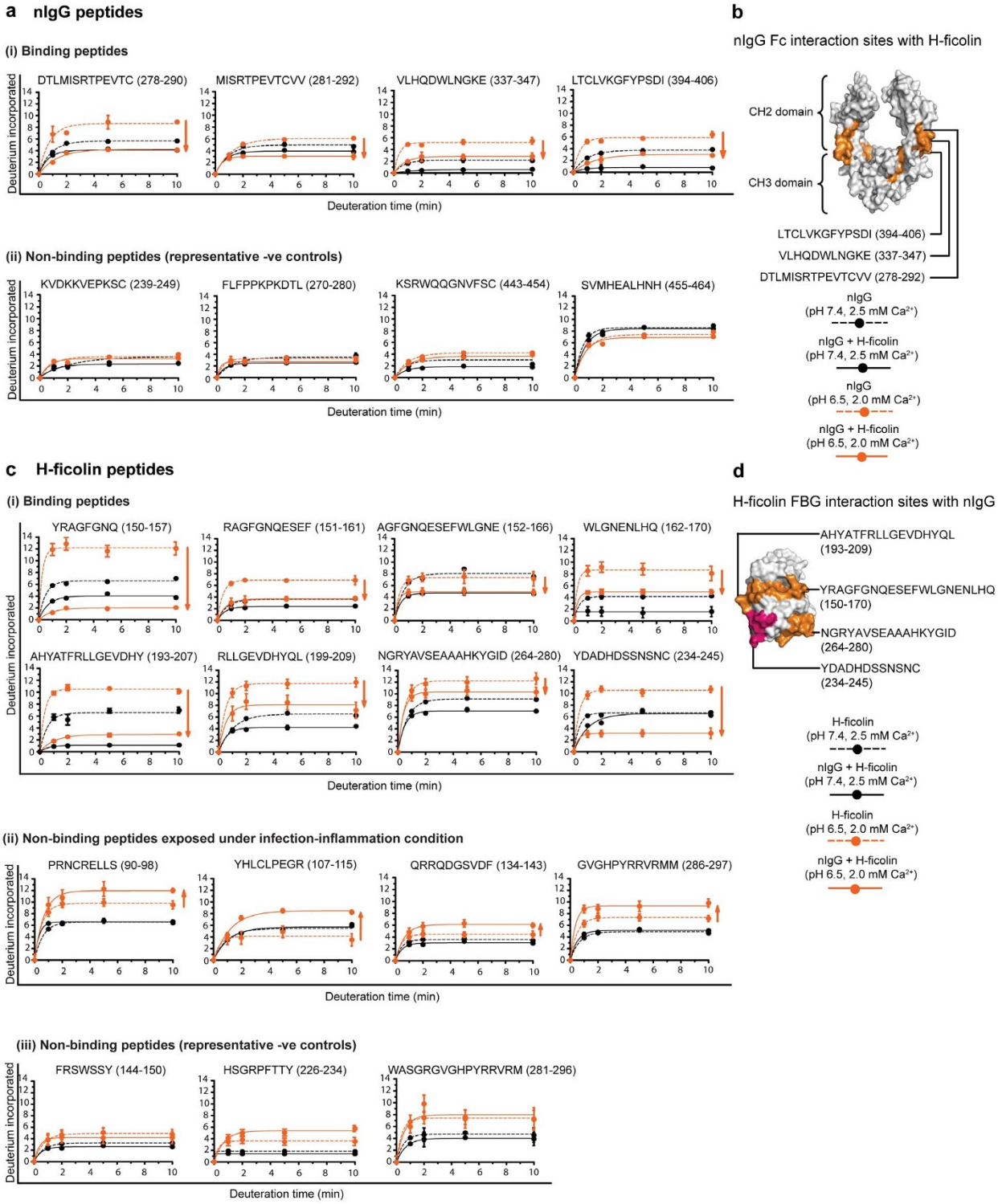


**Figure 4 | Identification of binding interfaces between nIgG and H-ficolin by HDMS.** (a) and (c) HDMS to identify interaction sites between (a) nIgG and (c) H-ficolin. Deuterium incorporation in proteins over time is annotated as follows: solid lines, presence of both nIgG and H-ficolin; dashed lines (control), presence of either nIgG or H-ficolin; black lines, normal condition; and orange lines, infection-inflammation condition. The amino acid sequence of the peptides is indicated in each panel. 18 and 16 peptides, respectively, of nIgG (70% coverage) and H-ficolin (85% coverage) were selected for plotting the graphs based on the mass spectrometric peak quality. Binding peptides of nIgG and H-ficolin showing decreased deuterium incorporation in the presence of both the proteins as compared to individual protein under both conditions, in particular under infection-inflammation condition are indicated by downward orange arrow. H-ficolin non-binding peptides showing increased deuterium incorporation in the presence of both proteins as compared to H-ficolin alone (under infection-inflammation condition) are indicated by upward orange arrow. Representative non-binding peptides showing no difference in deuterium incorporation in the presence of individual proteins or both proteins serve as negative controls. The structure diagrams indicate (b) nIgG Fc and (d) H-ficolin FBG, highlighting the interacting peptides in orange. The additional H-ficolin peptide ($YDADHDSSNSNC^{234-245}$) interacting with nIgG only under the infection-inflammation condition is highlighted in pink. Results are mean ± S.D. from 3 independent experiments.

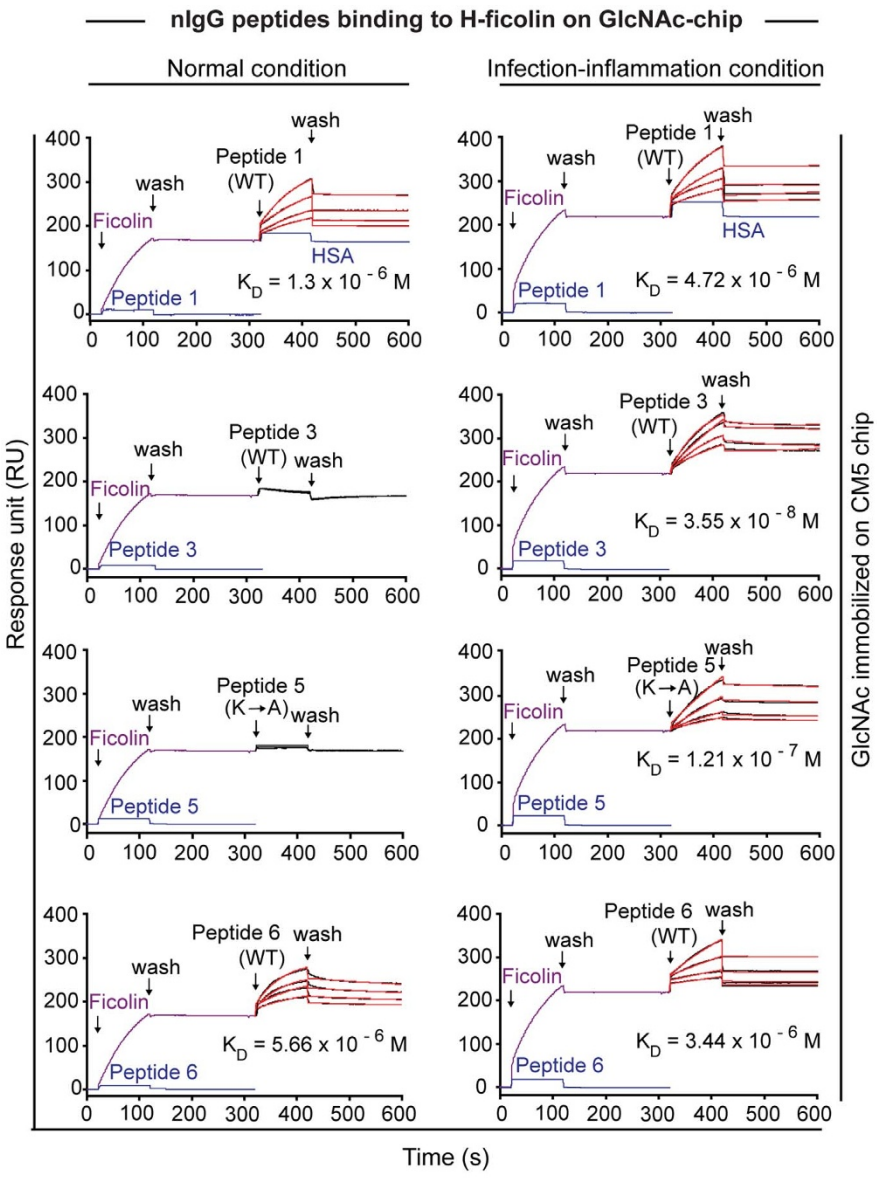


| nIgG Peptides | Sequence | Mutation | $K_D$ (M) Normal | $K_D$ (M) Infection-inflammation |
|---|---|---|---|---|
| 1 | $^{278}$DTLMISRTPEVTCVV$^{292}$ | WT | 1.3 x 10 - 6 | 4.72 x 10 - 6 |
| 2 | DTLMISATPEVTCVV | R → A | n.b. | n.b. |
| 3 | $^{337}$VLHQDWLNGKE$^{347}$ | WT | n.b. | 3.55 x 10 - 8 |
| 4 | VLAQDWLNGKE | H → A | n.b. | n.b. |
| 5 | VLHQDWLNGAE | K → A | n.b. | 1.21 x 10 - 7 |
| 6 | $^{394}$LTCLVKGFYPSDI$^{406}$ | WT | 5.66 x 10 - 6 | 3.44 x 10 - 6 |
| 7 | LTCLVAGFYPSDI | K → A | n.b. | n.b. |

n.b. refers to **non-binding** peptides where $K_D$ value could not be determined due to lack of binding, hence no curve-fitting was performed according to 1:1 Langmuir binding model. Non-binding mutant peptide data are not shown. Representative sensogram of non-binding peptides here are peptides 3&5 under normal condition.

**Figure 5 | Binding affinity and identification of contact residues of nIgG peptides with ficolin.** Surface plasmon resonance (response unit) to characterize the binding affinities between nIgG peptides and H-ficolin, under normal and infection-inflammation conditions. GlcNAc-BSA was immobilized on the CM5 chip to expose GlcNAc as a ligand for anchoring ficolin to the chip. H-ficolin (200 nM) was first injected over GlcNAc, respectively for 100 s (association time) followed by buffer flow (wash) for 200 s (dissociation time). Increasing concentrations of nIgG peptides (5, 10, 20 and 50 μM) were injected over the H-ficolin bound to the chip, under similar conditions. Mutant peptides (with Arg, Lys or His substituted to Ala) did not bind to the corresponding proteins. Human serum albumin (HSA) injected after H-Ficolin served as a negative control (blue, see top 2 panels). nIgG peptides (WT or mutants) are tabulated below the respective graphs. Peptides, injected directly over the GlcNAc-immobilized chip as controls, showed no binding to GlcNAc (blue). Data were analyzed using BIAevaluation software 3.2. The binding curves (black) are overlaid with the fit of 1 : 1 interaction model (red). The plots are a typical representation of 3 independent experiments.

increasing doses of the "ficolin-binding nIgG peptides". This is likely due to the competition between the "ficolin-binding IgG peptides" and whole nIgG to bind to ficolin. We still observed a significant increase in nIgG:ficolin complex formation under infection-inflammation condition compared to normal condition, with or without nIgG peptides. Since not all nIgG binding sites on the ficolin molecule are occupied by the peptides, it is conceivable that nIgG would bind with higher affinity to the unbound sites on ficolin under infection-inflammation condition, giving rise to an increase in nIgG:ficolin complexes. The binding of nIgG peptides to ficolin was specific since the non-binding nIgG peptides did not affect the formation of the nIgG:ficolin complex. In the absence of the bacterial mimic (-GlcNAc, Fig. 6a, bottom panel), no nIgG:ficolin complex was observed, indicating the specificity of immune complex formation only in presence of the bacteria.

To show the effects of pre-blocking ficolin in the serum on the formation of nIgG:ficolin complexes, we incubated the serum with nIgG peptides (which specifically target ficolin) compared with non-binding mutant nIgG peptides. Consistent with the ELISA results (Fig. 6a), we observed a significant reduction in nIgG:ficolin complexes in both human serum and pooled mice serum, when the sera were pre-treated with increasing doses of "ficolin-binding nIgG peptides" prior to incubating with *P. aeruginosa* (Fig. 6b). No effect on the complex formation was observed with sera incubated with control non-binding nIgG peptides, indicating the specific blocking of nIgG:ficolin interaction by the "ficolin-binding nIgG peptides". Recently, Panda et al provided further *in vivo* support by showing that the blocking of endogenous ficolin by the "ficolin-binding nIgG peptides" compromised the nIgG:ficolin immune complex formation during infection in mice and compromised their survival[12]. Taken together, these findings highlight the following: (a) the importance of specific interaction residues in the nIgG (Fig. 5), which when mutated, prevents interaction with ficolin, as evidenced by the inability of the mutant nIgG peptide to block the nIgG:ficolin interaction (Fig. 6b); (b) no nIgG:ficolin complexes were formed without infection, ascertaining the specificity of immune complex formation only upon infection to avoid random over-activation; (c) the significance of ficolin as a partner of nIgG, in facilitating the adaptive-innate immune crosstalk.

**nIgG:ficolin immune complexes are formed independently of C1q.** It is known that after IgG has formed immune complexes, C1q (a classical complement pathway activator) interacts with all isoforms of IgG at the CH2 domain of Fc, involving the residues: Glu 318, Lys 320 and Lys 322[30]. This IgG-C1q interaction then activates the classical complement pathway. Here, we have found that H-ficolin interacts with the CH2-CH3 domain interface of IgG (Fig. 4a, b). Next, we queried the potential involvement of C1q in the nIgG:ficolin immune complex formation. We first performed computational docking of known crystal structure of C1q on IgG Fc and observed that the binding site of C1q on IgG Fc (Supplementary fig. 3a) was consistent with previous finding[30]. Next, to test whether C1q and ficolin compete for binding to IgG during the immune complex formation, we superimposed the docking structures of C1q:IgG Fc (Supplementary fig. 3a) and of H-ficolin FBG:IgG Fc (Supplementary fig. 2b) on each other, and found that C1q and H-ficolin bind at different sites on IgG (Supplementary fig. 3b). Hence, C1q and ficolin may not compete with each other for IgG.

To further support the computational predictions, we tested the binding of C1q to immobilized nIgG (anti-alpha gal IgG from uninfected human serum) in the absence or presence of increasing doses of H-ficolin and vice versa. We found that C1q and H-ficolin were able to bind to nIgG to the same extent, independent of each other (Supplementary fig. 3c), further corroborating that C1q and ficolin bind to different sites on IgG Fc. Next, we tested whether C1q enables nIgG deposition on the bacterial mimic (GlcNAc beads) and if so, how it might influence the immune complex formation. We incubated the GlcNAc beads with H-ficolin or nIgG or C1q or a combination of these proteins, and observed that H-ficolin, which was bound to the bacterial mimic, did not recruit C1q, hence showing that C1q and H-ficolin did not interact. We found that C1q was recruited only after the nIgG:H-ficolin immune complex had formed and it did not influence the nIgG:ficolin mediated recognition of the bacterial mimic (Supplementary fig. 3d). This finding is consistent with reports that have shown that C1q is recruited by immobilized natural IgM after it had formed immune complexes[9,26]. Overall, these results indicate that C1q is not involved in nIgG:ficolin bacterial recognition and immune complex formation (Supplementary fig. 3e).

## Discussion

Collaboration between the two arms of immunity, wherein innate immunity directs the adaptive immune response, has been established as an important phenomenon in host defense against infection. Innate immune PRRs induce signals at multiple checkpoints[2,31] to dictate the initiation and control of the adaptive immune response. This is influenced by several parameters such as the origin and dose of the antigen, which impacts the type, magnitude and duration of the immune response and the production of long-term memory. Even though studies have shown that innate immunity shapes adaptive immunity, it is unclear whether and how the adaptive immune system affects the innate immune response. Our recent discovery that nIgG is not passive but plays an essential protective role during early infection by associating with ficolin bound to the pathogen[12], construes that an adaptive immune protein shapes the innate immune response. Here, we elucidated the biochemical and biophysical interaction between nIgG:ficolin and precisely mapped the functional domains and residues of contact between the two proteins.

We demonstrated increased nIgG:ficolin complex formation under mild acidosis and hypocalcaemia, which prevail at the site of infection. Studies with innate immune proteins have also highlighted similar higher affinity interactions under infection-inflammation condition[22], which leads to a synergistic immune response. Infection-induced reduction in pH is known to cause conformational changes in ficolin by exposing additional binding sites and enhancing its interaction with the acute phase protein, CRP[32,33]. The modulation of the immune response by varying pH and calcium levels suggests that the host makes use of these perturbations to regulate the pathogen recognition, immune complex formation and subsequent pathogen clearance. This phenomenon is crucial for the specificity of a pathogen-driven immune defense, precluding random immune response, which would otherwise result in autoimmunity. Importantly, we have revealed the precise sites of interaction between the two components of the adaptive and innate immune pathways under infection condition. Notably, we found an additional interaction binding site (YDADHDSSNSNC$^{234-245}$) in the ficolin which became exposed for interaction with nIgG under reduced pH and calcium levels, with a 100-fold increase in binding affinity (Fig. 5), possibly supporting the increase in the nIgG:ficolin complex formation. We also delineated the exact binding residues of IgG that interact with ficolin, and found that specific Arg ($R^{284}$) and Lys ($K^{346}$ and $K^{399}$) residues regulate the basal level of interaction under normal condition, whereas His ($H^{339}$) seems to be crucial in regulating the nIgG:ficolin interaction under infection condition. Other reports have also documented His to be a regulator of interaction between immune proteins under physiological and pathophysiological conditions[33]. At the pH of infection-inflammation condition used in our study, it is likely that the His side-chains undergo a change in their protonation states and adopt a more positive character at reduced pH. This change would be expected to impact the polar/ionic interactions between the two proteins and increase their affinity under the

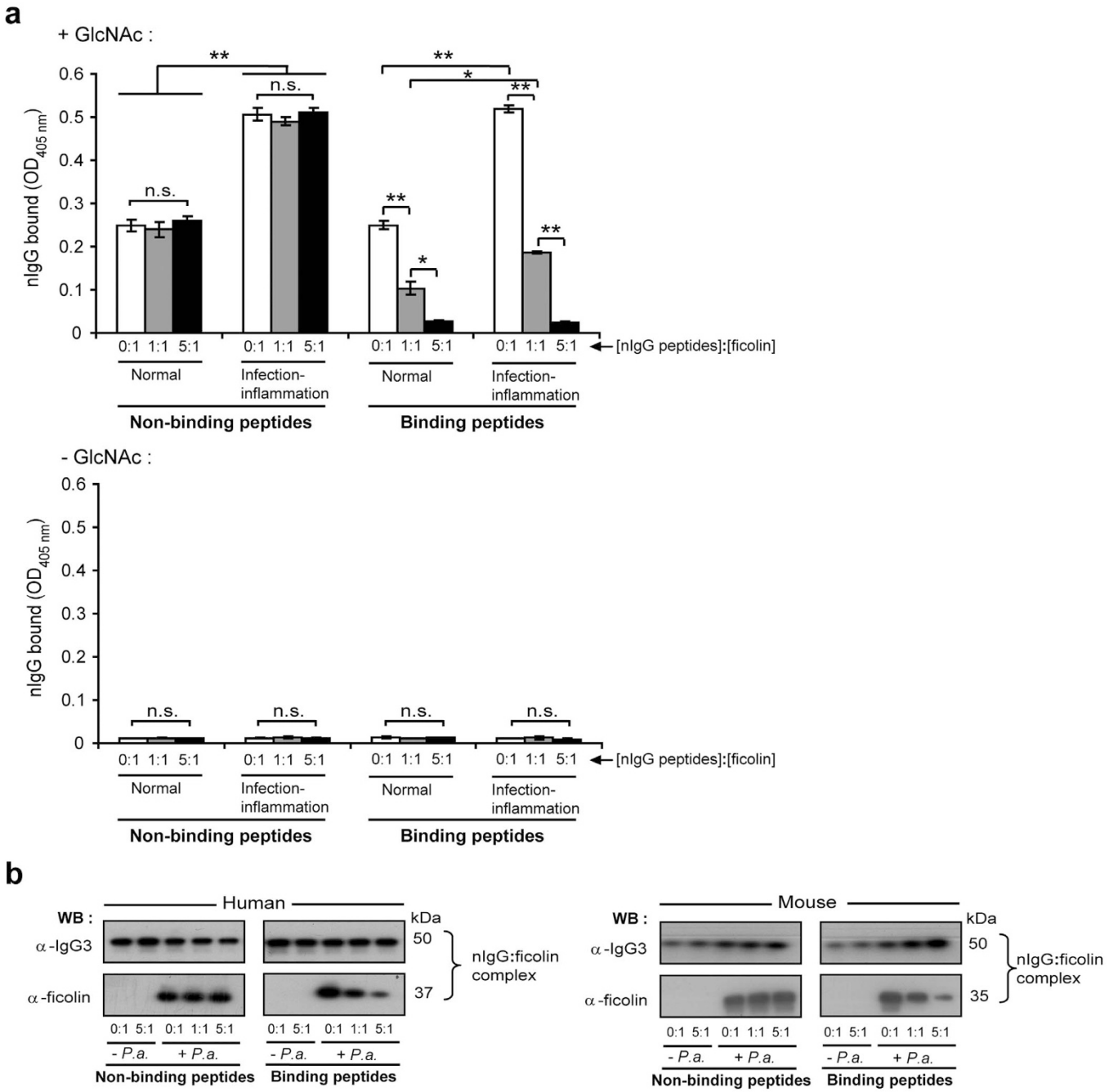


**Figure 6 | nIgG peptides (that bind ficolin) block nIgG:ficolin complex formation during infection.** (a) ELISA to detect binding of nIgG to H-ficolin pre-bound on immobilized GlcNAc under both normal and infection-inflammation conditions with or without prior incubation with nIgG binding and non-binding peptides to ficolin. Firstly, H-ficolin was incubated with immobilized GlcNAc-BSA (+GlcNAc), followed by increasing doses of nIgG peptides (non-binding or binding) in 1 : 1 or 5 : 1 molar ratio to H-ficolin. Then, 1 : 10 diluted ficolin-depleted serum was added and nIgG bound was detected using anti-human IgG3 and corresponding HRP-conjugated secondary antibody. BSA immobilized instead of GlcNAc-BSA (-GlcNAc) served as a negative control. Absorbance (OD) was read at 405 nm. Three replicates per condition were tested and three independent experiments were performed. $*p < 0.05$; $**p < 0.01$; n.s., not significant. (b) Immunoblot to detect nIgG (50 kDa heavy chain of IgG3) and ficolin (37 kDa; human and 35 kDa; mouse) in nIgG:ficolin complexes (pulled down by Protein G beads) in human serum and pooled mice sera (n = 8) upon incubation with *P. aeruginosa* (*P.a.*) for 30 min at room temperature. Prior to incubation with the bacteria, the sera were incubated with increasing doses of nIgG peptides (non-binding or binding to ficolin) for 15 min at room temperature. Sera pre-incubated without or with the peptides (5 : 1 molar ratio to ficolin) but without *P.a.* incubation, served as controls. The samples were derived from the same experiment, resolved under 12% reducing SDS-PAGE and the gels and blots were processed in parallel. Representative immunoblots (cropped for improving clarity and conciseness of presentation) from three independent experiments is shown. Full-length blots are presented in Supplementary Fig. 4b.

infection-inflammation condition. Additionally, we speculate that infection-induced conformational change in the ficolin FBG domain exposes extra sites to the solvent, which did not bind nIgG, but may engage with other serum proteins during infection. This would ensure interaction between multiple immune proteins to stage an optimal response against pathogens.

The ability of the host immune system to modulate the protein:-protein interactions by changes in the side-chain charge of amino

acids indicates immune regulation at the molecular level. In fact, the nIgG peptides that were found to bind ficolin were able to block nIgG:ficolin interaction to different extents depending on normal or infection-inflammation conditions. Hence, it is likely that these peptides have the potential to be developed into immunomodulators to treat immune disorders with impaired ficolin levels[4,5,34]. Furthermore, the potency of these peptides could be tuned by the prevailing pH and calcium conditions to modulate the immune complex formation.

Interestingly, the nIgG:ficolin immune complex formation takes place in a similar manner in both humans and mice, although ficolins from humans and mice differ in some of their physicochemical properties. Humans have three isoforms (L-, H- and M-), whereas mice have two isoforms – the mouse ficolins A and B are thought to be the respective homologues of human L-ficolin[35] and human M-ficolin[36]. The human H-ficolin is a pseudogene in mice[36]. However, we found that during infection, both the human and mice ficolins bind to the pathogen and recruit nIgG to form an immune complex. The conservation of this phenomenon across species suggests the fundamental significance of nIgG:ficolin mediated innate immune defense.

In our recent study[12], we found the important difference between nIgG (specifically belonging to the IgG3 subclass) and antigen-specific IgG3. Although both classes belong to the IgG3 subclass, they differ in the mode of bacterial recognition. Antigen-specific IgG is well-known to directly recognize and bind to the pathogen due to its specificity, whereas we found that nIgG requires the help of lectins like ficolin to recognize the bacteria. Once the immune complex is formed [bacteria GlcNAc:ficolin:IgG], it is likely that both nIgG and antigen-specific IgG will activate downstream pathways like complement activation and phagocytosis. Here, we also found that the nIgG:ficolin immune complex recruits C1q, which may subsequently activate the complement pathway. This novel shortcut mechanism of anti-microbial defense prompts further exploration in the field of natural antibodies and their role in immunity.

## Methods

**Mice.** 6–8 week old Balb/c mice were inbred in "specific pathogen free" conditions at the NUS CARE facility. Gender- and age-matched mice were used in the experiments. Systemic infection of the mice was performed intravenously through the tail vein. All experiments were carried out in compliance with institutional guidelines and approved by the Institutional Animal Care and Use Committee (IACUC Protocol Ref: 108/08).

**Analyses of protein binding by flow cytometry.** *P. aeruginosa* (PAO1 strain) was cultured and prepared for the experiment as previously described[12,22]. To estimate the binding of purified nIgG to bacteria, the bacteria were incubated with purified mouse nIgG with or without pooled mice serum depleted of IgG or depleted of both IgG and ficolin, for 2 h at room temperature, with shaking. The non-specific bound proteins were removed by washing three times with the wash buffers. Then, the nIgG bound was detected by staining the bacteria with primary anti-mouse IgG3 (1 : 500) (Sigma), followed by staining with corresponding Alexa 488-conjugated secondary antibody (1 : 500) (Invitrogen). Flow cytometric analysis was performed using Dako Cyan Cytomation LX (Becton Dickinson) and the samples were analyzed using the Summit V4.3.02 software.

**ELISA and Co-immunoprecipitation for analysis of H-ficolin, nIgG and C1q interactions.** ELISA was carried out as previously described[12,22], to test the interaction between nIgG:H-ficolin in the absence or presence of C1q or nIgG:C1q in absence or presence of H-ficolin. Information on the source of proteins used in the experiment is provided in the Supplementary information. Briefly, 1 μg of representative nIgG (human anti-alpha gal IgG) was immobilized overnight in 96-well Maxisorp™ plate (NUNC, Denmark) at 4°C, followed by co-incubation with 1 μg H-ficolin and increasing doses of C1q and vice versa, for 2 h at 37°C. After washing the wells four times with the wash buffers (TBST for normal condition or MBST for infection-inflammation condition), C1q or H-ficolin bound to nIgG was detected with respective primary anti-human C1q (1 : 2000) or anti-H-ficolin (1 : 3000) antibody followed by corresponding HRP-conjugated secondary antibody (1 : 3000). The ABTS substrate (Roche Diagnostics, Germany) was added to the wells and incubated in the dark for 15 min, followed by reading the absorbance at 405 nm.

To test for the immune complex formation between H-ficolin, nIgG and C1q on the bacterial mimic, GlcNAc beads (bacterial mimic) were incubated with H-ficolin, nIgG, C1q or a combination of the proteins under normal and infection-inflammation conditions for 2 h at room temperature. After washing the beads with the wash buffers, the proteins that had formed the immune complex on the bacterial mimic were detected by boiling the GlcNAc beads in 1× SDS-PAGE loading dye, followed by analysis using SDS-PAGE electrophoresis and Western blotting using specific antibodies.

**Immunohistochemistry of spleen sections.** Mice were euthanized, and spleen tissues were procured, washed in PBS and immediately frozen in Jung tissue freezing medium (Leica Microsystems) using liquid nitrogen, in a similar manner as previously described[12]. Tissues were sectioned at a thickness of 5 μm using Leica Cryostat 1850. For immunohistochemistry, the spleen sections were fixed with 4% paraformaldehyde and stained with primary antibodies (anti-mouse IgG3 and anti-ficolin) and respective secondary antibodies. Imaging was done using LSM 510 Meta confocal microscope.

**Cell cultures.** The U937 monocytic cell line was cultured in RPMI 1640 (Invitrogen) supplemented with 10% (v/v) FBS (Invitrogen), 100 IU/ml penicillin and 100 μg/ml streptomycin (Invitrogen) at 37°C, 5% $CO_2$ condition. HEK293T cells expressing the recombinant proteins (transfected with the pSecTag2 recombinant vectors) were cultured in DMEM (Invitrogen) supplemented with 10% FBS, 100 IU/ml penicillin, 100 μg/ml streptomycin and 200 μg/ml zeocin (selection antibiotic).

**Simulation of "normal" and "infection-inflammation" conditions *in vitro*.** The infection-inflammation condition is characterized by a drop in pH from 7.4 to 6.5[37] at the infection site. The calcium concentration in the infected tissue microenvironment has also been reported to drop to ≤2 mM from 2.2 to 2.6 mM in the healthy condition[19–21]. Therefore, we simulated "normal condition" (TBS buffer containing 25 mM Tris, 145 mM NaCl, pH 7.4 and 2.5 mM $CaCl_2$) and "infection-inflammation condition" (MBS buffer containing 25 mM MES, 145 mM NaCl, pH 6.5 and 2 mM $CaCl_2$) using the specific buffers, similar to what has been previously used by others[22–24].

**Immunofluorescence staining.** For detecting the co-localization of the proteins on the monocyte surface, U937 monocytes were plated at a density of $0.5 \times 10^6$ cells/ml onto charged coverslips. Then, the monocytes were incubated with the GlcNAc-beads pre-incubated with proteins for 20 min at 37°C, washed thrice with PBS and fixed with 4% paraformaldehyde for 15 min at room temperature. Non-specific staining of the monocytes was blocked by incubating in the blocking buffer (3% BSA in PBS) for 30 min at room temperature. The monocytes were then incubated with the respective primary and secondary antibodies diluted in the incubation buffer (3% BSA in PBS containing 0.05% Tween 20) for 60 min at room temperature and washed thrice with PBS containing 0.05% Tween 20. The nucleus was stained using Prolong Gold antifade reagent with DAPI (Invitrogen) present in the mounting media. Images were taken by the LSM META 510 confocal microscope (Carl Zeiss) using a 63× oil objective.

***In situ* proximity ligation assay.** Proximity ligation assay (PLA) was performed to quantitate the nIgG:ficolin interactions *in situ*, as described earlier[12]. Briefly, $0.5 \times 10^6$ U937 monocytes were first plated onto charged cover slips (Sterilin, London, UK). The monocytes were then incubated with GlcNAc-beads pre-opsonized with H-ficolin or, nIgG or both the proteins for 20 min at 37°C under simulated normal or infection-inflammation conditions. Monocytes were washed three times with PBS, fixed with 4% (w/v) paraformaldehyde in PBS for 15 min, followed by blocking with 10% fetal bovine serum in PBS for 2 h at room temperature. The nIgG:ficolin complexes were detected using compatible primary antibodies and secondary antibodies conjugated with PLUS and MINUS oligonucleotide probes [Duolink detection 563 kit (Olink Biosciences, Uppsala, Sweden)]. The oligonucleotides present in the two PLA probes hybridize only if they are in close proximity (eg. during protein:protein interaction). Subsequently, the two hybridized oligonucleotides were ligated by Duolink ligase, amplified by Duolink Polymerase and detected as red fluorescent signals using LSM 510 Meta Confocal Laser Scanning microscope (Carl Zeiss). All images were taken using a 63× oil immersion lens. Samples incubated without primary antibodies served as experimental negative controls.

**Amide hydrogen-deuterium exchange mass spectrometry (HDMS) and data analysis.** HDMS was performed to delineate the interaction interfaces between nIgG and H-ficolin under normal (pH 7.4) and infection-inflammation (pH 6.5) conditions. The experimental protocol followed was similar to that described by Zhang et al[32]. Briefly 2 μl each of the both the proteins (concentrations approx. 2.5 mg/ml) were mixed with 18 μl of the deuterated buffer at the pH 7.4 or 6.5, in order to start the hydrogen-deuterium exchange reaction. After incubating the reaction mixture for different time points (0, 1, 2, 5, or 10 min) to allow the hydrogen-deuterium exchange, the reaction was quenched by lowering the pH to 2.5 with the addition of 180 μl of ice-cold 0.1% (v/v) trifluoroacetic acid (Sigma-Aldrich). Then, 100 μl of the quenched reaction mixture was mixed with 50 μl pepsin bead slurry (Pierce) to enable protein digestion. The pepsin beads were activated by washing thrice with 0.1% trifluoroacetic acid (pH 2.5) at 4°C. The pepsin-added reaction mixture was vortexed for 30 s and incubated on ice for 30 s, and this cycle was carried out for 5 min. The hydrogen-deuterium exchanged mixture was then clarified by centrifuging at 7000 g for 1 min at 4°C. The supernatant was divided into three fractions, quickly frozen in liquid nitrogen, and stored at −80°C.

Mass spectrometry of the pepsin-digested protein samples was performed using the 4800 Plus MALDI TOF/TOF Analyzer (Applied Biosystems, Foster City, CA). In case any deuterium back-exchange occurred during the experiment, we included control reactions where the exchange was carried out for 24 h at 25°C in nIgG or H-ficolin alone and the data were calculated accordingly. The resulting mass spectra were viewed and calibrated using the Data Explorer version 4.9 software (Applied Biosystems). The data were analyzed with reference to the theoretical mass of the two prominent peptides in the spectra (theoretical m/z = 932.42 and 1452.73). Peptide mass (average value) was calculated by determining the centroid of its isotopic envelope using the Decapp software (University of California San Diego, La Jolla, CA). The average number of deuterium atoms incorporated in the peptide was calculated based on the difference between its centroid values in the deuterated and non-deuterated samples. Hydrogen-deuterium exchange at the side chains was determined to be in 4.5% of the fast-exchanging side-chain hydrogen atoms based on the dilution factors. The side-chain deuteration factor was corrected prior to the back-exchange correction during data analysis. Kinetic graphs of deuterium incorporation in the peptides were plotted with the best fit based on a single exponential model accounting for deuterium atoms that were exchanged at a fast rate (mainly with the amide hydrogen atoms that were exposed to the solvent) during the reaction. Graphs with best fit were plotted using the GraphPad Prism version 5 (GraphPad Software, San Diego, CA). The difference in deuterium incorporation in the peptides between the individual protein (nIgG or H-ficolin) and the complex (nIgG:H-ficolin), that were greater or lesser than 10%, were considered as significant[38].

**Real-time biointeraction analysis.** To demonstrate the interaction between peptide and protein in real-time, we employed surface plasmon resonance (SPR) analysis using the BIAcore 2000 instrument (BIAcore AB), as previously described[12]. Briefly, we first immobilized the CM5 chip with 10 μg/ml GlcNAc-BSA (Dextra Labs, UK) in 10 mM sodium acetate (pH 4.0) using the amine-coupling chemistry, according to the manufacturer's specifications. Next, H-ficolin (200 nM) in running buffer was injected over the GlcNAc-immobilized chip for 100 s (association) followed by buffer flow for 200 s (dissociation). To characterize the binding of nIgG peptides to H-ficolin, separate second injections of increasing concentrations of nIgG peptides were made under similar running conditions. During the experiment, the flow rate was constantly maintained at 30 μl/min. The bound proteins were removed after one cycle by injecting 15 μl of 0.1 M NaOH (regeneration buffer).

We used specific buffers for simulating the "normal condition" with TBS buffer (25 mM Tris, 145 mM NaCl, pH 7.4, 2.5 mM $CaCl_2$) and the "infection-inflammation condition" with MBS buffer (25 mM MES, 145 mM NaCl, pH 6.5, 2 mM $CaCl_2$). The SPR sensograms were analyzed by the BIAevaluation 3.2 software and the $K_D$ (dissociation constant) was calculated using 1 : 1 Langmuir binding model. The plots were finally made by overlaying the original binding curves (black) with the 1 : 1 binding model fitted curves (red). Controls used for normalization were obtained by injection of buffers alone instead of the proteins. The difference in the value of the resonance unit before and after injection is a measure of the peptide:protein interaction. The plots shown are representative of three independent experiments.

**Statistical analysis.** For all the experiments, three replicates were performed per sample/condition tested. Data are presented as mean ± SEM of three independent experiments. Differences between averages were analyzed by two-tailed Student's t test. Significance was set at $p$ value of $< 0.05$. *$p < 0.05$; **$p < 0.01$; n.s. not significant.


1. Medzhitov, R. & Janeway Jr, C. A. Innate immunity: the virtues of a nonclonal system of recognition. *Cell* **91**, 295–298 (1997).
2. Palm, N. W. & Medzhitov, R. Pattern recognition receptors and control of adaptive immunity. *Immunological reviews* **227**, 221–233, doi:10.1111/j.1600-065X.2008.00731.x (2009).
3. Malhotra, R. *et al.* Glycosylation changes of IgG associated with rheumatoid arthritis can activate complement via the mannose-binding protein. *Nature medicine* **1**, 237–243 (1995).
4. Arnold, J. N. *et al.* Human serum IgM glycosylation: identification of glycoforms that can bind to mannan-binding lectin. *The Journal of biological chemistry* **280**, 29080–29087, doi:10.1074/jbc.M504528200 (2005).
5. Royle, L. *et al.* Secretory IgA N- and O-glycans provide a link between the innate and adaptive immune systems. *J Biol Chem* **278**, 20140–20153, doi:10.1074/jbc.M301436200 (2003).
6. Notkins, A. L. Polyreactivity of antibody molecules. *Trends Immunol* **25**, 174–179, doi:10.1016/j.it.2004.02.004 (2004).
7. Zhou, Z. H. *et al.* The broad antibacterial activity of the natural antibody repertoire is due to polyreactive antibodies. *Cell host & microbe* **1**, 51–61, doi:10.1016/j.chom.2007.01.002 (2007).
8. Ochsenbein, A. F. *et al.* Control of early viral and bacterial distribution and disease by natural antibodies. *Science* **286**, 2156–2159 (1999).
9. Ehrenstein, M. R. & Notley, C. A. The importance of natural IgM: scavenger, protector and regulator. *Nature reviews. Immunology* **10**, 778–786, doi:10.1038/nri2849 (2010).
10. Boyden, S. V. Natural antibodies and the immune response. *Advances in immunology* **5**, 1–28 (1966).
11. Michael, J. G. Natural antibodies. *Current topics in microbiology and immunology* **48**, 43–62 (1969).
12. Panda, S., Zhang, J., Tan, N. S., Ho, B. & Ding, J. L. Natural IgG antibodies provide innate protection against ficolin-opsonized bacteria. *The EMBO journal* **32**, 2905–2919, doi:10.1038/emboj.2013.199 (2013).
13. Galili, U., Buehler, J., Shohet, S. B. & Macher, B. A. The human natural anti-Gal IgG. III. The subtlety of immune tolerance in man as demonstrated by crossreactivity between natural anti-Gal and anti-B antibodies. *The Journal of experimental medicine* **165**, 693–704 (1987).
14. Perlmutter, R. M., Hansburg, D., Briles, D. E., Nicolotti, R. A. & Davie, J. M. Subclass restriction of murine anti-carbohydrate antibodies. *Journal of immunology* **121**, 566–572 (1978).
15. Puga, I. & Cerutti, A. Protection by natural IgG: a sweet partnership with soluble lectins does the trick! *The EMBO journal* **32**, 2897–2899, doi:10.1038/emboj.2013.235 (2013).
16. Bessman, A. N., Page, J. & Thomas, L. J. In vivo pH of induced soft-tissue abscesses in diabetic and nondiabetic mice. *Diabetes* **38**, 659–662 (1989).
17. Baranov, D. & Neligan, P. Trauma and aggressive homeostasis management. *Anesthesiology clinics* **25**, 49–63, viii, doi:10.1016/j.atc.2006.11.003 (2007).
18. Zar, T., Yusufzai, I., Sullivan, A. & Graeber, C. Acute kidney injury, hyperosmolality and metabolic acidosis associated with lorazepam. *Nature clinical practice. Nephrology* **3**, 515–520, doi:10.1038/ncpneph0573 (2007).
19. TranVan Nhieu, G., Clair, C., Grompone, G. & Sansonetti, P. Calcium signalling during cell interactions with bacterial pathogens. *Biology of the cell/under the auspices of the European Cell Biology Organization* **96**, 93–101, doi:10.1016/j.biolcel.2003.10.006 (2004).
20. Prince, A. S., Mizgerd, J. P., Wiener-Kronish, J. & Bhattacharya, J. Cell signaling underlying the pathophysiology of pneumonia. *American journal of physiology. Lung cellular and molecular physiology* **291**, L297–300, doi:10.1152/ajplung.00138.2006 (2006).
21. Eichstaedt, S. *et al.* Effects of Staphylococcus aureus-hemolysin A on calcium signalling in immortalized human airway epithelial cells. *Cell calcium* **45**, 165–176, doi:10.1016/j.ceca.2008.09.001 (2009).
22. Zhang, J. *et al.* Local inflammation induces complement crosstalk which amplifies the antimicrobial response. *PLoS Pathog* **5**, e1000282, doi:10.1371/journal.ppat.1000282 (2009).
23. Miyazawa, K. & Inoue, K. Complement activation induced by human C-reactive protein in mildly acidic conditions. *J Immunol* **145**, 650–654 (1990).
24. Gu, Q. & Lee, L. Y. Characterization of acid signaling in rat vagal pulmonary sensory neurons. *Am J Physiol Lung Cell Mol Physiol* **291**, L58–65, doi:10.1152/ajplung.00517.2005 (2006).
25. Ochsenbein, A. F. & Zinkernagel, R. M. Natural antibodies and complement link innate and acquired immunity. *Immunol Today* **21**, 624–630 (2000).
26. Holmskov, U., Thiel, S. & Jensenius, J. C. Collections and ficolins: humoral lectins of the innate immune defense. *Annual review of immunology* **21**, 547–578, doi:10.1146/annurev.immunol.21.120601.140954 (2003).
27. Matsushita, M., Endo, Y., Hamasaki, N. & Fujita, T. Activation of the lectin complement pathway by ficolins. *International immunopharmacology* **1**, 359–363 (2001).
28. Hoofnagle, A. N., Resing, K. A. & Ahn, N. G. Protein analysis by hydrogen exchange mass spectrometry. *Annu Rev Biophys Biomol Struct* **32**, 1–25, doi:10.1146/annurev.biophys.32.110601.142417 (2003).
29. Mandell, J. G., Falick, A. M. & Komives, E. A. Measurement of amide hydrogen exchange by MALDI-TOF mass spectrometry. *Anal Chem* **70**, 3987–3995 (1998).
30. Duncan, A. R. & Winter, G. The binding site for C1q on IgG. *Nature* **332**, 738–740, doi:10.1038/332738a0 (1988).
31. Iwasaki, A. & Medzhitov, R. Toll-like receptor control of the adaptive immune responses. *Nat Immunol* **5**, 987–995, doi:10.1038/ni1112 (2004).
32. Zhang, J. *et al.* Secreted M-ficolin anchors onto monocyte transmembrane G protein-coupled receptor 43 and cross talks with plasma C-reactive protein to mediate immune signaling and regulate host defense. *Journal of immunology* **185**, 6899–6910, doi:10.4049/jimmunol.1001225 (2010).
33. Zhang, J., Yang, L., Anand, G. S., Ho, B. & Ding, J. L. Pathophysiological condition changes the conformation of a flexible FBG-related protein, switching it from pathogen-recognition to host-interaction. *Biochimie* **93**, 1710–1719, doi:10.1016/j.biochi.2011.06.003 (2011).
34. Andersen, T., Munthe-Fog, L., Garred, P. & Jacobsen, S. Serum levels of ficolin-3 (Hakata antigen) in patients with systemic lupus erythematosus. *J Rheumatol* **36**, 757–759, doi:10.3899/jrheum.080361 (2009).
35. Kwon, S. *et al.* Identification of a functionally relevant signal peptide of mouse ficolin A. *Journal of biochemistry and molecular biology* **40**, 532–538 (2007).
36. Endo, Y. *et al.* Identification of the mouse H-ficolin gene as a pseudogene and orthology between mouse ficolins A/B and human L-/M-ficolins. *Genomics* **84**, 737–744, doi:10.1016/j.ygeno.2004.07.006 (2004).
37. Martinez, D. *et al.* Extracellular acidosis induces neutrophil activation by a mechanism dependent on activation of phosphatidylinositol 3-kinase/Akt and ERK pathways. *J Immunol* **176**, 1163–1171 (2006).

38. Schuster, M. C. *et al.* Dynamic structural changes during complement C3 activation analyzed by hydrogen/deuterium exchange mass spectrometry. *Mol Immunol* **45**, 3142–3151, doi:10.1016/j.molimm.2008.03.010 (2008).

## Acknowledgments

We thank the Ministry of Education (Tier 1 grant: WBS R-154-000-584-112 and Tier 2 grant: T208B3109) and A*STAR BMRC (Grant: 10/1/21/19/658) for supporting this research. Saswati Panda is a graduate research scholar of the National University of Singapore. Zhang Jing is an NGS scholar. Yang Lifeng is a research fellow of the Singapore-MIT Alliance (Computational Systems Biology Programme). We are grateful to Mazlina Banu for technical help.

## Author contributions

S.P. designed, performed and analyzed the experiments in this study with intellectual input from J.L.D. J.Z. provided advice in designing *in vitro* experiments. L.Y. conducted the computational studies. G.S.A. provided advice in analyzing HDMS data. J.L.D. provided overall coordination with respect to conception, design and supervision of the study. S.P., J.Z. and J.L.D. wrote the manuscript with comments from co-authors.

## Additional information

**Supplementary information** accompanies this paper at http://www.nature.com/scientificreports

**Competing financial interests:** The authors declare no competing financial interests.

**How to cite this article:** Panda, S., Zhang, J., Yang, L.F., Anand, G.S. & Ding, J.L. Molecular interaction between natural IgG and ficolin – mechanistic insights on adaptive-innate immune crosstalk. *Sci. Rep.* **4**, 3675; DOI:10.1038/srep03675 (2014).